

Improved Two-Phase Projection Topology Optimization

Josephine V. Carstensen and James K. Guest

Department of Civil Engineering, Johns Hopkins University, Baltimore, MD 21218, USA

jvcarstensen@jhu.edu, jkguest@jhu.edu

1. Abstract

Projection-based algorithms for continuum topology optimization have received considerable attention in recent years due to their ability to control minimum length scale in a computationally efficient manner. This not only provides a means for imposing manufacturing length scale constraints, but also circumvents numerical instabilities of solution mesh dependence and checkerboard patterns. Standard radial projection, however, imposes length scale on only a single material phase, potentially allowing small-scale features in the second phase to develop. This may lead to sharp corners and/or very small holes when the solid (load-carrying) phase is projected, or one-node hinge chains when only the void phase is projected. Two-phase length scale control is therefore needed to prevent these potential design issues. Ideally, the designer would be able to impose different minimum length scales on both the structural (load-carrying) and void phases as required by the manufacturing process and/or application specifications. A previously proposed algorithm towards this goal required a design variable associated with each phase to be located at every design variable location, thereby doubling the number of design variables over standard topology optimization [2]. This work proposes a two-phase projection algorithm that remedies this shortcoming. Every design variable has the capability to project either the solid or the void phase, but nonlinear, design dependent weighting functions are created to prevent both phases from being projected. The functions are constructed intentionally to resemble level set methods, where the sign of the design variable dictates the feature to be projected. Despite this resemblance to level sets, the algorithm follows the material distribution approach with sensitivities computed via the adjoint method and MMA used as the gradient-based optimizer. The algorithm is demonstrated on benchmark minimum compliance and compliant inverter problems, and is shown to satisfy length scale constraints imposed on both phases.

2. Keywords: Topology Optimization, Projection Methods, Manufacturing Constraints, Length Scale, Heaviside Projection.

3. Introduction

Topology optimization is a design tool used for determining optimal distributions of material within a domain. System connectivity and feature shapes are optimized and thus, as the initial guess need not be informed, topology optimization is capable of generating new and unanticipated designs. It is well-known, however, that this may result in impractical solutions that are difficult to fabricate or construct, such as ultra slender structural features or small scale pore spaces. A key focus of this work is to improve manufacturability of topology-optimized designs by controlling the length scale of the topological features.

The length scale is generally defined as the minimum radius or diameter of the material phase of concern. It is thus a physically meaningful quantity that can be selected by the designer based on fabrication process. The fabrication process also dictates the phase (or phases) on which the restriction is applied. For example, for topologies constructed by deposition processes, it is relevant to consider constraining the minimum length scale of the solid phase. Similarly, for designs that are manufactured by removing material, for example by milling, the manufacturability constraints should include minimum length scale and maximum curvature of the voids as dictated by the machine. Moreover, it is well established that controlling the length scale has the additional advantage that it circumvents numerical instabilities, such as checkerboard patterns and mesh dependency.

Several methods for controlling the length scale of a topology optimization design exist ([1], [3]). Herein, the Heaviside Projection Method (HPM) [1] is used. HPM is capable of yielding 0-1 designs in which the minimum length scale is achieved naturally, without additional constraints. In HPM, the design variables are associated with a material phase and projected onto the finite element space by a Heaviside function. This mathematical operation is independent of the problem formulation and the governing physics. The projection is typically done radially and the projection radius is chosen as the prescribed minimum length scale. In its original form [1], the method projects a single phase onto the elements and

hence length scale control is only achieved for that phase. Undesirable features have been seen to appear in the alternate, non-controlled phase. This includes small scale voids and sharp corners when the solid phase is projected and ultra-thin structural members when only the void phase is projected.

In [2] it was proposed to control the minimum length scale of multiple phases independently by having multiple sets of design variables - one for each phase. All the design variables are projected independently onto the finite elements and combined to obtain the final topology, typically using a standard intermediate density penalization scheme to satisfy the conditions on the design variables. While this seemed to perform well, the primary disadvantage of the approach was that the number of design variables increased by a factor of two. Although this could be mitigated using sparse design variable fields (e.g. [4]), this property was generally undesirable.

In this paper, we propose to controlling the minimum length scale of multiple phases of a design by letting a single design variable pass through a nonlinear weighting function that determines which phase to project. This idea was recently proposed in Reference [5] where negative design variables indicated void projection and positive solid design variables. The weighting functions, however, required three parameters that, for some problems, required significant tuning. Our goal here is to develop a more stable algorithm.

4. Review of Heaviside Projection Method using multiple phase projection

The basis of the proposed algorithm is the multiple phase projection implementation of the Heaviside Projection Method (HPM) ([2]). This implementation uses multiple sets of design variables and is briefly reviewed here. The design variables are denoted ϕ_p and two material phases are considered and referred to as $p = s$ and $p = v$ for solid and void, respectively.

From the perspective of the elements, each element receives projected phase from any design variable within a distance r_{min} of the element centroid $\bar{\mathbf{x}}^e$. This information is stored in the neighborhood set N^e for the element, formally defined as

$$i \in N^e \quad \text{if } \|\mathbf{x}_i - \bar{\mathbf{x}}^e\| \quad (1)$$

where \mathbf{x}_i is the location of design variable i .

The mapping onto the finite elements is done by first computing the weighted average of the design variables in the set N^e for each element. This is done for all actively projected phases using that the following standard equation for weighted average $\mu_p^e(\phi)$:

$$\mu_p^e(\phi) = \frac{\sum_{i \in N^e} w(\mathbf{x}_i - \bar{\mathbf{x}}^e) \cdot \{\phi_p\}_i}{\sum_{i \in N^e} w(\mathbf{x}_i - \bar{\mathbf{x}}^e)} \quad (2)$$

where $w(\mathbf{x}_i - \bar{\mathbf{x}}^e)$ is a linear weighting function that scales the information received by each design variable according to the design variable location. Typically either a uniform or a linear weighting function is used.

To obtain binary solutions, nonlinear projection is used where the average design variables μ_p^e are passed through a regularized Heaviside function to obtain the element volume fraction ρ_p^e for each phase. As for single phase projection, the element volume fractions for the solid and the void phase are defined as follows:

$$\rho_s^e(\phi) = 1 - e^{-\beta \mu_s^e(\phi)} + \mu_s^e(\phi) e^{-\beta} \quad (3)$$

$$\rho_v^e(\phi) = e^{-\beta \mu_v^e(\phi)} - \mu_v^e(\phi) e^{-\beta} \quad (4)$$

Here $\beta \geq 0$ dictates the curvature of the regularization which approaches the Heaviside function as β approaches infinity.

The element volume fractions $\rho_e(\phi)$ are assembled by averaging the element volume fractions from projected phase.

$$\rho^e(\phi) = \frac{\rho_s^e(\phi) + \rho_v^e(\phi)}{2} \quad (5)$$

Note that an element is a solid element if and only if solid phase is actively projected onto the element ($\mu_s^e > 0, \rho_s^e = 1$) and void is not projected ($\mu_v^e = 0, \rho_v^e = 1$). Likewise a void element is achieved if and only if solid phase is not actively projected onto the element ($\mu_s^e = 0, \rho_s^e = 0$) and void is actively projected ($\mu_v^e > 0, \rho_v^e = 0$). Intermediate volume fractions result when both phases are projected (termed

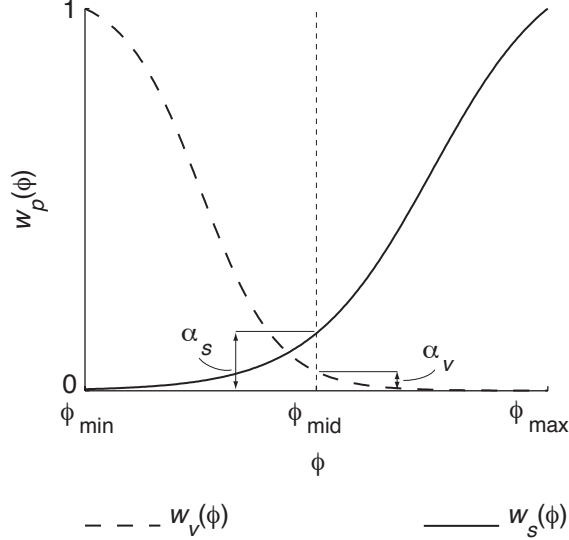


Figure 1: Illustration of the weighting functions $w_s(\phi)$ and $w_v(\phi)$ in the interval ϕ_{min} to ϕ_{max} for $\alpha_s = 0.15$ and $\alpha_v = 0.05$.

phase mixing) or when neither are actively projected (termed passive regions). The reader is referred to [2] for images and additional details.

5. Multiple phase projection using nonlinear weighting functions

In this work, we propose using a nonlinear weighing function to indicate the actively projected phase, rather than use multiple sets of design variables. The weighted average of the design variables for each element $\mu^e(\phi)$ is now computed using

$$\mu_p^e(\phi) = \frac{\sum_{i \in N^e} w(\mathbf{x}_i - \bar{\mathbf{x}}^e) \cdot w_p(\phi_i)}{\sum_{i \in N^e} w(\mathbf{x}_i - \bar{\mathbf{x}}^e)} \quad (6)$$

where $w_p(\phi)$ is the nonlinear, design variable dependent functions that serve as projection indicators. For the solid phase, the function values ranges from close to zero for the minimum value of the design variable, ϕ_{min} , to 1 at the maximum value ϕ_{max} . Similarly, the function value of void weighting function ranges from 1 at ϕ_{min} to close to zero at ϕ_{max} . At the mid of the range of the design variables, ϕ_{mid} , the weighting function equals the constant α_p , that is chosen for each phase such that $\alpha_p \in (0, 1]$. Herein, the nonlinear weighting functions are taken as the hyperbolic tangent as illustrated in Fig. 1. The functions are defined by

$$w_s(\phi) = \frac{1 + \alpha_s}{1 + \alpha_s \cdot e^{2n_s(\phi_{max} - \phi)}} \quad (7)$$

$$w_v(\phi) = \frac{1 + \alpha_v}{1 + \alpha_v \cdot e^{2n_v(\phi - \phi_{min})}} \quad (8)$$

where $\phi_{range} = \phi_{max} - \phi_{min}$ and

$$n_p = -\frac{2 \ln(\alpha_p)}{\phi_{range}} \quad (9)$$

As noted in the Introduction, Reference [5] used a similar idea with $\phi_{mid} = 0$, $\phi_{min} = -1$, and $\phi_{max} = 1$. These parameter magnitudes were intentionally selected to mimic level set methods, and are used here again with the hyperbolic tangent function. Examining Figure 1, it can be seen that negative ϕ magnitudes will lead to void projection and the creation of void features, while positive ϕ magnitudes indicate solid projection and creation of solid features.

5.1 Penalization of intermediate values

The element stiffness matrices are related to topology using the Solid Isotropic Material with Penalization

(SIMP) method ([7], [8]) and the elemental stiffness matrix is therefore expressed as

$$\mathbf{K}^e(\phi) = (\rho^e(\phi)^\eta + \rho_{min}^e) \mathbf{K}_0^e \quad (10)$$

where $\eta \geq 1$ is the exponent penalty term, \mathbf{K}_0^e is the stiffness matrix of a pure solid element and ρ_{min}^e is a small positive number to maintain positive definiteness of the global stiffness matrix. Herein, $\rho_{min}^e = 10^{-4}$ is used for elastic design problems.

5.2 Sensitivities

The sensitivities of the objective function are calculated as follows:

$$\frac{\partial f}{\partial \phi_i} = \sum_{e \in \Omega} \frac{\partial f}{\partial \rho^e} \frac{\partial \rho^e}{\partial \phi_i} \quad (11)$$

The partial derivative of the objective function f with respect to the element volume fraction ρ^e is problem dependent and calculated using the adjoint method. The partial derivative of the element volume fraction with respect to the design variables follows the chain rule. By differentiating Eq.(3), Eq.(4) and Eq.(5) the following expression is found:

$$\frac{\partial \rho^e}{\partial \phi_i} = \frac{1}{2} \left[\left(\beta e^{-\beta \mu_s^e(\phi)} + e^{-\beta} \right) \frac{\partial \mu_s^e}{\partial \phi_i} - \left(\beta e^{-\beta \mu_v^e(\phi)} + e^{-\beta} \right) \frac{\partial \mu_v^e}{\partial \phi_i} \right] \quad (12)$$

where the partial derivatives of μ_s^e and μ_v^e are found by differentiating Eq.(6) for $p = s$ and $p = v$, respectively.

6. Example Problems and Solution Algorithms

The proposed algorithm is evaluated on the benchmark minimum compliance and compliant mechanism design problems.

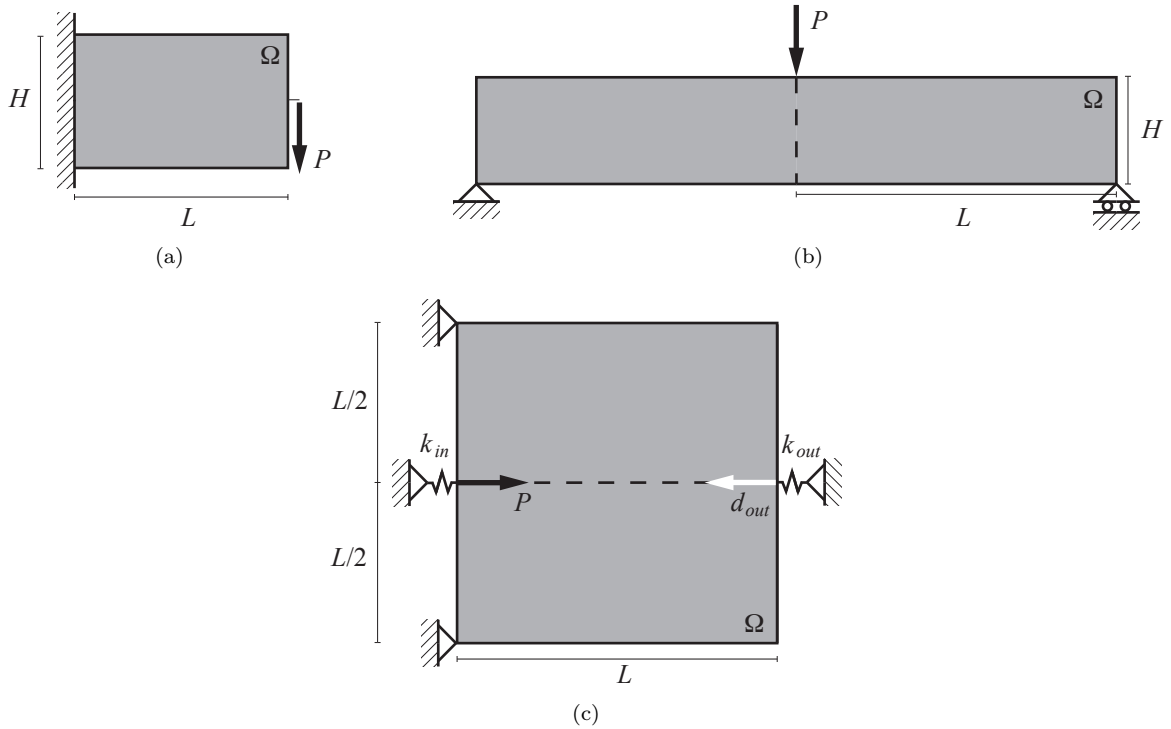


Figure 2: (a) The cantilever beam problem and (b) the MBB beam problem, both optimized for minimum compliance, and (c) the compliant mechanism design problem where the objective is to maximize the displacement at the output port (d_{out}) for input force P .

6.1 Minimum compliance problem

The optimization formulation for minimum compliance may in general be written as

$$\begin{aligned} & \text{minimize} && \mathbf{F}^T \mathbf{d} \\ & \text{subject to} && \mathbf{K}(\phi) \mathbf{d} = \mathbf{F} \\ & && \sum_{e \in \Omega} \rho^e(\phi) v^e \leq V \\ & && \phi_{min} \leq \phi_i \leq \phi_{max} \quad \forall i \in \Omega \end{aligned} \quad (13)$$

where \mathbf{F} are the nodal forces, \mathbf{d} are the nodal displacements and \mathbf{K} is the global stiffness matrix. The allowable volume of material is denoted V and v^e is the volume of element e . The design variable bounds are $\phi_{min} = -1$ and $\phi_{max} = 1$ as in [5].

The minimum compliance problem is self-adjoint and hence it follows that the derivative of the objective function f with respect to the element volume fraction ρ^e is

$$\frac{\partial f}{\partial \rho^e} = -\eta(\rho^e(\phi))^{\eta-1} \mathbf{d}^{eT} \mathbf{K}_0^e \mathbf{d}^e \quad (14)$$

The minimum compliance problem is solved for both the cantilever and the MBB beam problems (Fig. 2a and Fig. 2b). The cantilever problem has $L = 40$, $H = 25$ and $P = 1$, whereas the MBB problem has $L = 60$, $H = 20$ and $P = 1$. For both problems, a volume constraint of $V = 0.50$ is used and, for the MBB beam problem, only the right half of the domain is designed.

6.2 Compliant inverter design

For inverter compliant mechanism design, the optimization formulation is given as

$$\begin{aligned} & \text{minimize} && \mathbf{L}^T \mathbf{d} \\ & \text{subject to} && \mathbf{K}(\phi) \mathbf{d} = \mathbf{F} \\ & && \sum_{e \in \Omega} \rho^e(\phi) v^e \leq V \\ & && \phi_{min} \leq \phi_i \leq \phi_{max} \quad \forall i \in \Omega \end{aligned} \quad (15)$$

where \mathbf{L} is a vector with value one at the entry associated with the output point displacement degree of freedom and zeros at all other locations.

The derivative of the objective function with respect to the element volume fraction ρ^e is found using the adjoint method as follows:

$$\frac{\partial f}{\partial \rho^e} = -\eta(\rho^e(\phi))^{\eta-1} \lambda^{eT} \mathbf{K}_0^e \mathbf{d}^e \quad (16)$$

where λ^e is the elemental component of the vector λ , found by solving the FE problem $\mathbf{K}(\phi) \lambda = \mathbf{L}$.

For the inverter design problem (Fig. 2c), only the bottom half of the domain is designed with $L = 120$, $P = 1$, $V = 0.25$ and $k_{in} =$ and $k_{out} = 10^{-3}$.

6.3 Optimizer

All problems are solved using the Method of Moving Asymptotes (MMA) as the optimization algorithm ([6], [9]). MMA is widely used in topology optimization as it efficiently handles a large number of design variables provided there are few constraints. A continuation method is applied to the SIMP exponent penalty to transform the problem from a relaxed, unpenalized state to the penalized, near discrete formulation. This is common practice in topology optimization as it is known to help avoid convergence to undesirable local minima. Herein, we use $\Delta\eta = 1.0$ and $\eta_{max} = 5.0$. No continuation is applied to the Heaviside parameter [10], and a constant value of $\beta = 50$ is taken throughout. The reader is referred to [1] for detailed algorithmic steps. All problems are solved using four node quadrilateral elements, a uniform initial distribution of material, and $\phi_{min} = -1$ and $\phi_{max} = 1$. Elasticity problems assume plane stress conditions with Young's modulus and Poisson's ratio of 1.0 and 0.3, respectively.

7. Results

7.1. Minimum compliance problems

The solutions to the MBB beam problem with a prescribed minimum length scale of $r_{min} = 1.00$ are given in Fig. 3 for solid only, void only, and the proposed two-phase projection formulation on a 240×80 mesh. The overall topology is the same, but there are differences in the topological details. Acute angles are seen when only solid projection is used (Fig. 3a), whereas using only void projection results in much rounder junctions (Fig. 3b). However, it is clearly seen that the length scale control of the solid phase is

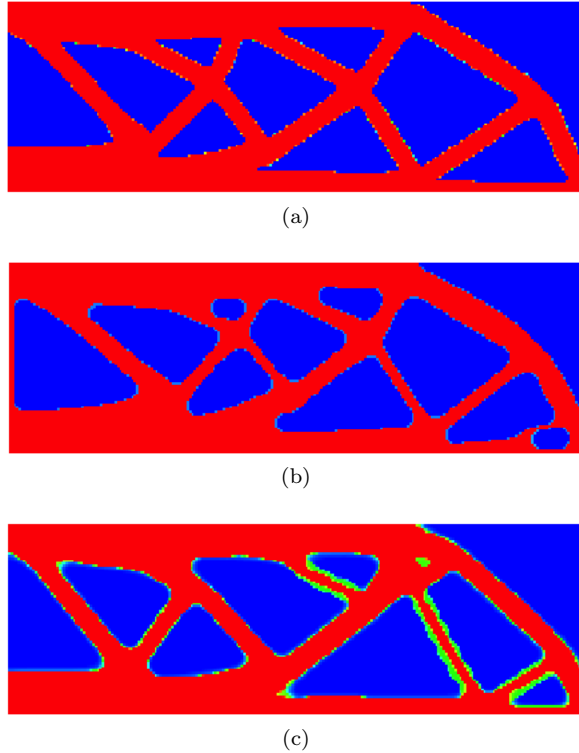


Figure 3: MBB beam with $r_{min} = 1.00$ applied to (a) solid phase only, (b) void phase only, and (c) solid and void phase using the new approach with $\alpha_s = 0.001$ and $\alpha_v = 0.0005$.

lost when using only void projection and that very slender members can therefore occur. The two-phase projection allows control of both phases using the current algorithm. As Fig. 3c indicate, the drawback of these methods is that they appear to have slightly more intermediate volume fractions than the single phase solutions.

The results for the cantilever problem using the proposed algorithm is given in Fig. 4 on a 80×50 and a 240×150 mesh with a prescribed minimum length scale of both phases of $r_{min} = 0.50$. It is clearly seen that mesh independence is achieved for this problem.

7.2 Compliant mechanism design problem

The results of the inverter compliant mechanism are given for single phase projection in Fig. 5a for solid projection and Fig. 5b for void projection, and for the new two-phase projection approach in Fig. 5c,d. It is seen that the new approach creates slightly more intermediate volume fractions in the regions of the hinge. This is ultimately due to phase mixing and the relatively large magnitudes of the selected r_{min} .

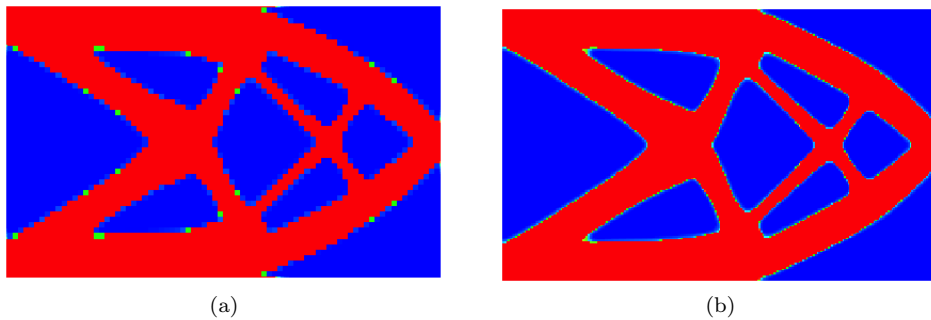


Figure 4: Cantilever with $r_{min} = 0.50$ applied to both phases on a (a) 80×50 mesh, and a (b) 240×150 mesh.

When the minimum length scale of the void phase is decreased to $r_{min} = 2.00$, facilitating tighter packing of the projections, the amount of intermediate volume density around the hinges are seen to decrease slightly (Fig. 5d).

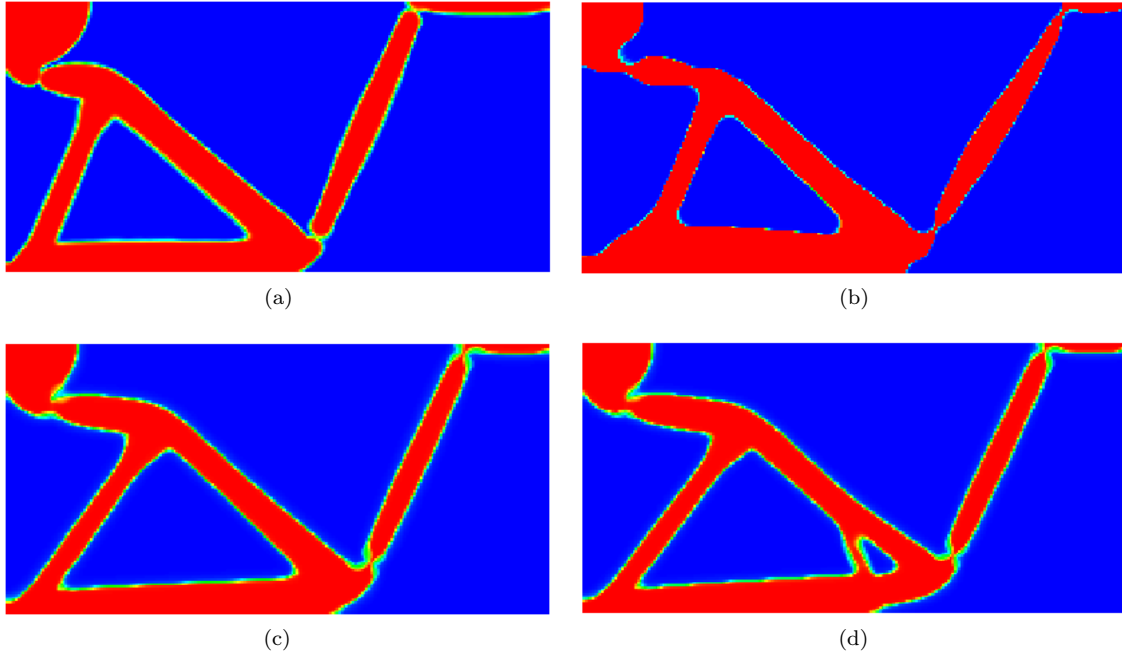


Figure 5: Force inverter with $r_{min} = 2.50$ applied to (a) solid phase only, (b) void phase only, and solid and void phase using the new approach with $\alpha_s = 0.002$ and $\alpha_v = 0.0005$ with (c) solid and void phase length scales of $r_{min} = 2.50$ and (d) solid phase length scale of $r_{min} = 2.50$ and void phase length scale of $r_{min} = 2.00$.

7. Conclusion

A technique is proposed for restricting the minimum length scale of multiple phases in topology optimization. This allows the designer to prescribe a minimum allowable length scale for both the solid (structural) phase and the void phase, and these length scales need not be equivalent. This is achieved by actively projecting both solid and void phases from each design variable. This is in contrast to our previous work ([2]) which used independent design variables associated with each specific phase, thereby doubling the number of design variables. The effect is achieved here using nonlinear weighting functions. These weighting functions are structured such that the design variable magnitude indicates whether solid phase or the void phase is actively projected by the design variable. This maintains constant dimensionality of the design variable space, while allowing active projection and therefore length scale control of both phases. The disadvantage of the proposed approach is that the weighting functions are now design variable dependent and nonlinear. This could potentially make it more challenging for the optimizer to identify quality solutions, although our preliminary results indicate this is not necessarily the case.

8. References

- [1] J.K. Guest, J.H. Prévost and T. Belytschko, Achieving minimum length scale in topology optimization using nodal design variables and projection functions, *Int. J. Numer. Meth. Engng.*, 61 (2), 238-254, 2004.
- [2] J.K. Guest, Topology optimization with multiple phase projection, *Comput. Methods Appl. Mech. Engrg.*, 199 (1-4), 123-135, 2009.
- [3] O. Sigmund, Morphology-based black and white filters for topology optimization, *Struct. Multidisc. Optim.*, 33 (4), 401-424, 2007.

- [4] J.K. Guest, and L. Smith Genut, Reducing dimensionality in topology optimization using adaptive design variable fields, *Int. J. Numer. Meth. Engng.*, 81 (8), 1019-1045, 2010.
- [5] J.K. Guest, Improved projection-based algorithms for continuum topology optimization, *Collection of Technical Papers - 13th AIAA/ISSMO Multidisciplinary Analysis and Optimization Conference*, Fort Worth, TX, 1-9, 2010.
- [6] K. Svanberg, The method of moving asymptotes - a new method for structural optimization, *Int. J. Numer. Meth. Engng.*, 24, 359-373, 1987.
- [7] M.P. Bendsøe, Optimal shape design as a material distribution problem, *Struct. Optim.*, 1, 193-202, 1989.
- [8] G.I.N. Rozvany, M. Zhou and T. Birker, Generalized shape optimization without homogenization, *Struct. Optim.*, 4, 250-252, 1992.
- [9] K. Svanberg, A globally convergent version of MMA without linesearch, *1st World Congress on Structural and Multidisciplinary Optimization*, G.I.N. Rozvany, N. Olhoff (Eds.), WCSMO, Goslar, Germany, 9-16, 1995.
- [10] J.K. Guest, A. Asadpoure and S. Ha, Eliminating beta-continuation from Heaviside projection and density filter algorithms, *Struct. Multidisc. Optim.*, 44 (4), 443-453, 2011.